4f spin driven ferroelectric-ferromagnetic multiferroicity in $PrMn_2O_5$ under a magnetic field

Chattopadhyay, S.; Balédent, V.; Panda, S. K.; Yamamoto, S.; Duc, F.; Herrmannsdörfer, T.; Uhlarz, M.; Gottschall, T.; Mathon, O.; Wang, Z.;

Originally published:

September 2020

Physical Review B 102(2020), 094408

DOI: https://doi.org/10.1103/PhysRevB.102.094408

Perma-Link to Publication Repository of HZDR:

https://www.hzdr.de/publications/Publ-31512

$4f$-spin driven ferroelectric-ferromagnetic multiferroicity in $PrMn_2O_5$ under magnetic field

S. Chattopadhyay,[1,*] V. Balédent,[2] S. K. Panda,[3] Sh. Yamamoto,[1] F. Duc,[4] T. Herrmannsdörfer,[1] M. Uhlarz,[1] T. Gottschall,[1] O. Mathon,[5] Z. Wang,[6] C. Strohm,[7] M. Greenblatt,[8] P. Foury-Leylekian,[2] and J. Wosnitza[1,9]

[1]*Dresden High Magnetic Field Laboratory (HLD-EMFL), Helmholtz-Zentrum Dresden-Rossendorf, 01328 Dresden, Germany*
[2]*Laboratoire de Physique des Solides, CNRS, Université Paris-Sud, Université Paris-Saclay, 91405 Orsay Cedex, France*
[3]*Department of Physics, Bennett University, Greater Noida 201310, Uttar Pradesh, India*
[4]*Laboratoire National des Champs Magnétiques Intenses (UPR 3228 CNRS, INSA, UJF, UPS) 143 avenue de Rangueil, F-31400 Toulouse, France*
[5]*European Synchrotron Radiation Facility, B.P. 220, 38043 Grenoble, France*
[6]*Anhui Province Key Laboratory of Condensed Matter Physics at Extreme Conditions, High Magnetic Field Laboratory of the Chinese Academy of Sciences, Hefei 230031, China*
[7]*Deutsches Elektronen-Synchrotron DESY, 22607 Hamburg, Germany*
[8]*Department of Chemistry and Chemical Biology, Rutgers, The State University of New Jersey, Piscataway, New Jersey 08854, USA*
[9]*Institut für Festkörper- und Materialphysik, Technische Universität Dresden, 01062 Dresden, Germany*

(Dated: January 21, 2020)

In contrast to all other members of the RMn_2O_5 family with non-zero $4f$ electrons (R = Nd to Lu), $PrMn_2O_5$ does not show any spin-driven ferroelectricity in the magnetically ordered phase. By means of high-field electric polarization measurements up to 45 T, we have found that this exceptional candidate too undergoes a spin-driven multiferroic phase under magnetic field. X-ray magnetic circular dichroism study up to 30 T at the Pr L_2-edge shows that this ferroelectricity is originated from and directly coupled to the ferromagnetic component of the Pr^{3+} spins. Experimental observations along with our GGA+U calculations reveal that this exotic coupled ferroelectric-ferromagnetic combination stabilizes through the exchange-striction mechanism solely driven by a $3d$-$4f$ type coupling, as opposed to the other RMn_2O_5 members with $3d$-$3d$ driven ferroelectric-antiferromagnetic type conventional type-II multiferroicity.

The research on functional materials, aiming at the next generation smart-devices, witnessed a massive upturn after the advent of materials with multiple coupled properties. Among such materials, an exotic family of compounds known as magnetoelectric multiferroics (MEMF) with coupled magnetism and ferroelectricity has been one of the key attractions [1–3]. For the MEMF family, reasons for being so highly sought after are twofold: (i) The microscopic origin of the magnetoelectric coupling is an intriguing question that fascinates the condensed matter community and (ii) from an applied perspective, the spintronics and data storage technologies would greatly benefit from such functionalities. However, to be well suited for device-applications, MEMF materials must fulfill two foremost criteria: ferromagnetism coexisting with ferroelectricity, and a strong coupling between the two order parameters. In reality, it is extremely difficult to satisfy both the criteria simultaneously. Multiferroic materials have been classified into two types. In type-I, ferroelectricity and magnetism have different origins leading to a weak coupling between them. Whereas in type-II multiferroics, spin driven ferroelectricity (SDFE) is caused by magnetic ordering itself, resulting an intrinsically strong magnetoelectric coupling [3–5]. However, the magnetism being frustrated in character, type-II multiferroics contain coexistence of complex antiferromagnetism and ferroelectricity. As multiferroics are relatively scarce, an important research activity focuses on heterostructures with stacked ferromagnetic (F) and ferroelectric layers [3] as well. However, as it eventually lead to type-I artificial multiferroics, the inconvenience of having small-coupling remains unsolved.

In this context, studies on RMn_2O_5 (R = Y, Bi, rare-earth) type oxides are particularly interesting. The RMn_2O_5 family is known for showing a series of magnetic transitions of nearly generic characters starting from R = Nd to Lu. The first magnetic transition around 40±5 K is incommensurate antiferromagnetic (AF) and is followed by a second transition leading to a commensurate AF ordering of the Mn spins. An electric polarization (P) concurrently emerges with this second magnetic transition along the b-axis, asserting the type-II character of the multiferroicity[6–15]. The associated strong-coupling has been reported for $GdMn_2O_5$ and $TbMn_2O_5$ where the electric polarization (P) can even be reversed by applying a modest magnetic field of a few Tesla [1, 2, 16, 17]. With lowering of temperature, a third magnetic transition generally appears stabilizing another incommensurate AF order. Neutron diffraction studies indicate that this spin-driven P is in general a consequence of a quasi-collinear ordering of the Mn spins (either Mn^{3+} sub-lattice or both Mn^{3+} and Mn^{4+} sub-lattices) [6, 7, 9]. To be noted, although the actual room-temperature crystal structure of RMn_2O_5 is already polar with a Pm (monoclinic) space group [18], the structural distortion with respect to the average non-polar $Pbam$ space group [19, 20] is so small that the induced polarization becomes extremely weak and can not be measured directly in this regime. We will thus neglect this weak symmetry breaking in the following.

In RMn_2O_5, the long standing debate on the microscopic origin of the SDFE has been resolved recently confirming Mn-

Mn exchange-striction to be the responsible one [7]. This result portrays the dominant role of 3d ions and their frustrated superexchange interactions in the emergence of SDFE. However, presence of a weak 3d-4f superexchange coupling (J_6) has also been proposed to understand the spin-structure evolution in some candidates [21, 22]. Particularly in $GdMn_2O_5$ (Neutron diffraction study) and $NdMn_2O_5$ (Raman and IR spectroscopy), in addition to the dominant 3d-3d effect, a weak 3d-4f interaction was proposed to be an additional parameter to explain the observed SDFE [10, 23]. It is noteworthy that 4f elements are quite well known for their exotic electric properties and their usage in permanent magnets. Therefore, a proper understanding of their coupling to the 3d ions could pave the way in designing highly functional materials eventually leading towards ferroelectric-ferromagnetic multiferroics with strong electromagnetic coupling. To gain insight about the coupling, it would be highly beneficial to have a system where the SDFE would dominantly/solely be driven by the 3d-4f mechanism.

Among all compositions, $PrMn_2O_5$ appears to be an interesting exception. In contrast to the other RMn_2O_5 members with non-zero numbers of 4f electrons, $PrMn_2O_5$ does not show any SDFE. Powder neutron diffraction measurements show that Mn^{3+} moments order at T_{N1} = 25 K following a magnetic propagation vector q_1 = (0.5, 0, 0). With decreasing temperature, Mn^{4+} ordering appears at T_{N2} = 18 K with q_2 = (0, 0, 0.5). Such distinct orderings of Mn^{3+} and Mn^{4+} are indicative of very weak exchange coupling between the two sub-lattices, explaining the absence of ferroelectricity. Pr^{3+} sub-lattice does not get fully ordered down to 1.5 K. Only a partial ordering of Pr^{3+} below T_{N1} was reported [24] suggesting a coupling (J_6) between Mn^{3+} and Pr^{3+}. Powder neutron study under high pressure (a few GPa) shows emergence of a collinear magnetic phase favorable for SDFE [25]. However, polarization measurements were not possible to perform at this pressure regime to probe the possible onset of multiferroicity directly.

In this Letter, we report the emergence of a multiferroic phase under magnetic field in $PrMn_2O_5$. Using the combination of high-field electric polarization, x-ray magnetic circular dichroism (XMCD), and density functional theory (DFT) based calculations, we show that unlike the multiferroicity observed in other RMn_2O_5 members, the SDFE in $PrMn_2O_5$ is originated from and coupled to a ferromagnetic component. Moreover, the associated mechanism involved is no longer based on the 3d-3d coupling, rather the SDFE is solely a manifestation of 3d-4f exchange interaction.

Single crystals of $PrMn_2O_5$ from the same batch as mentioned in reference [18] were used for this study. The crystals were grown using electrolysis method as described in references [26, 27]. The as-grown crystals have a thin plate-like morphology with the plate-surface being perpendicular to the b-axis. Specific-heat (C) measurements show two characteristic transitions at T_{N1} = 19 K and T_{N2} = 16 K. It is lower than the ones reported for the powder sample. However, such a discrepancy between the single crystal and powder has already been observed in $NdMn_2O_5$ due to the difference in the degree of frustration [6]. In addition to the specific-heat measurements, detailed magnetization (M) measurements were performed by applying the field along a, b, and c axes. The results are coherent with the powder neutron diffraction study performed earlier. Detailed results of specific-heat and magnetization measurements could be found in the Supplemental Information (SI).

We carried out high-field $P(H)$ measurements up to 45 T using pyroelectric technique (see SI for details) at the Dresden High Magnetic Field Laboratory (HLD-EMFL). Field pulses of ~20 ms duration were applied along b to measure the spin-induced pyroelectric-current (I) along the same direction. Electric-polarization was then calculated by integrating the $I(H)$ curves. In the $P(H)$ data shown in Fig. 1, it is evident that at 1.5 K, a spontaneous P emerges above ~12 T along the b direction. It increases with H and attains its maximum value around 27 T. With further increase in field, P decreases slowly and finally enters to a flat region above 35 T. Notably, the polarization amplitude in $PrMn_2O_5$ (~1 nC/cm^2) is of the same order as found in $NdMn_2O_5$, the adjacent member. The polarization gradually becomes weaker at higher temperatures and finally vanishes in the paramagnetic regime.

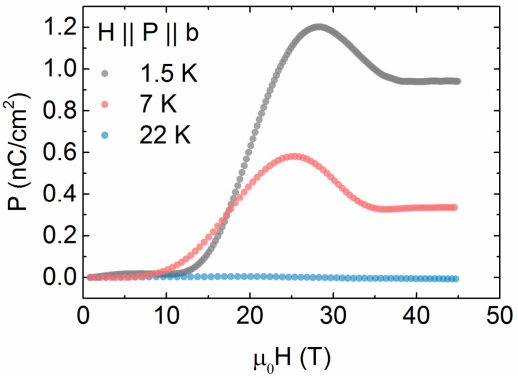

FIG. 1. Electric polarization (P) along the b-axis as a function of magnetic field showing the field-induced ferroelectricity.

In order to investigate the effect of a strong magnetic field on the rare earth ordering, we performed x-ray-magnetic-circular-dichroism (XMCD) measurements with same temperature and field conditions used for polarization. The high-field XMCD measurements at Pr-L_2 edge were performed at the energy dispersive x-ray absorption spectroscopy beamline ID24 at ESRF, Grenoble [28]. Magnetic fields up to 30 T along the beam direction were produced by a pulsed magnet [29, 30]. XMCD spectra were obtained in transmission mode at 2 K as the difference of x-ray absorption spectra when changing the field direction (+b and -b). The same measurement protocol was applied for both right- and left-handed circularly polarized x-ray beam. The field-dependence of the absorption spectrum was recorded through a multi-frame detection scheme [31]. For our purpose, the crystal was mounted with the b-axis parallel to the magnetic field

and incident beam direction. The polished sample (thinned down to ∼15 μm) was sandwiched between two diamond windows. This assembly was mounted in a dynamic He-flow cryostat in which the sample was cooled down through forced convection. Fig. 2 shows XMCD spectra recorded at some representative magnetic fields between 13 T and 30 T. The main contribution at the L_2-edge comes from the $2p_{1/2} \rightarrow 5d_{3/2}$ dipole transition according to the selection rules. As the magnetic field increases, the XMCD amplitude becomes more pronounced. The observed x-ray absorption spectra (See Fig. S4 in SI) and dichroic spectra at the high-field regime are consistent with those reported for other Pr^{3+} based systems ($4f^2$) [32, 33]. The dichroic signal starts to appear from ∼10 T, reaches its maximum around 27 T, and then drops gradually with further increase in H. Although we cannot entirely exclude the contribution from the Mn ions, the Pr L_2-edge XMCD signal observed in $PrMn_2O_5$ is contributed mainly by the Pr spins. The direct evidence could be seen from the peak-shape of the XMCD signal. It does not change with the field, only its amplitude gets modified unlike the garnet [35, 36] oxides, where the L-edge XMCD line-shape as well as amplitude change with field due to contributions of comparable strength from both $4f$ and $3d$ ions. In case of inter-metallic compounds composed of a $4f$ rare-earth and a $3d$ transition-metal, earlier study reported a sizable transition-metal contribution as well to the rare-earth L_2-edge [34]. This is because the $3d$-$4f$ exchange interaction in such inter-metallic compounds is mediated by the rare-earth $5d$ band which is directly accessed by the rare-earth L-edge. Instead, in our system, super-exchange type weaker $3d$-$4f$ interaction is mediated via the oxygen $2p$ state, which gives marginal transition-metal contribution to the XMCD signals at the rare-earth L-edges. Here, the mixed $4f$-$5d$ state of the Pr^{3+} is the reason the transition toward $5d_{3/2}$ gives access to the $4f$ spin's ferromagnetic ordering. As a consequence, these results prove that the Pr ions present a ferromagnetic component along the b axis under an external magnetic field applied along the same axis.

Notably, the field dependence of the integrated XMCD signal has a remarkable resemblance with the aforementioned $P(H)$ curve. In order to compare them, we represented in Fig. 3 the field dependence of both integrated XMCD signal and polarization at comparable temperature (2 K for XMCD and 1.5 K for P). It appears then as a striking evidence that the two order parameters are coupled. The direct consequence is that $PrMn_2O_5$ becomes a type-II multiferroic under magnetic field, coupling ferromagnetism and ferroelectricity.

In order to provide further credence to our experimental findings, we carried out density functional theory (DFT) calculations including Hubbard U and spin-orbit coupling (SOC) within the framework of GGA+U approach. The obtained spin and orbital angular momentum of Pr^{3+} ions are respectively 1.81 μ_B and 1.99 μ_B and they are in opposite directions. The spin moment on Pr^{3+} is large as expected from the nominal charge state (f^2). However the presence of strong reverse orbital moment makes the net moment very small (0.18 μ_B) which agrees with the neutron result (∼0.5 μ_B). The moment

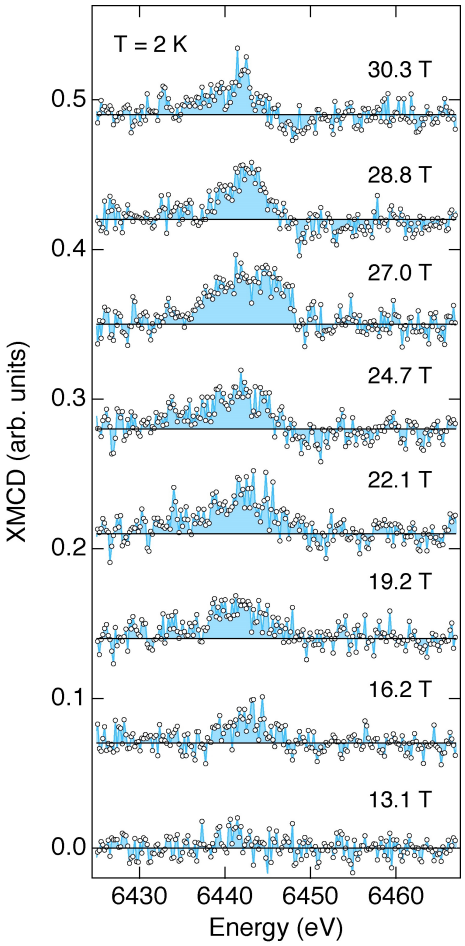

FIG. 2. Selected high-field x-ray magnetic circular dichroism (XMCD) spectra at the Pr L_2-edge with magnetic field applied parallel to the b-axis at T = 2 K. Data sets for different magnetic fields are offset along the vertical axis for clarity.

of Mn^{3+} and Mn^{4+} are essentially spin moments with the estimated values 3.38 and 2.55 μ_B respectively. Further, to set-up a spin-model for understanding the field dependence of polarization and its relation with the long range magnetic ordering, we estimated the inter-atomic magnetic exchange interactions from the converged GGA+U calculations using the formalism of Ref.[37]. In this method, we mapped the total converged energies of the magnetic system onto the following Heisenberg type spin Hamiltonian

$$\hat{H} = -\sum_{i \neq j} J_{ij} \vec{S_i} \cdot \vec{S_j} \quad (1)$$

Here, the indices i and j span over the positions of the intrinsically magnetic ions i.e. Pr^{3+}, Mn^{3+} and Mn^{4+}. The effective J_{ij} is extracted in a linear-response manner via a Green's function technique. A detailed discussion of the electronic structure and adopted computational methods are given in SI.

The estimated exchange interactions are listed in Table I. These results are fully compatible with the known mag-

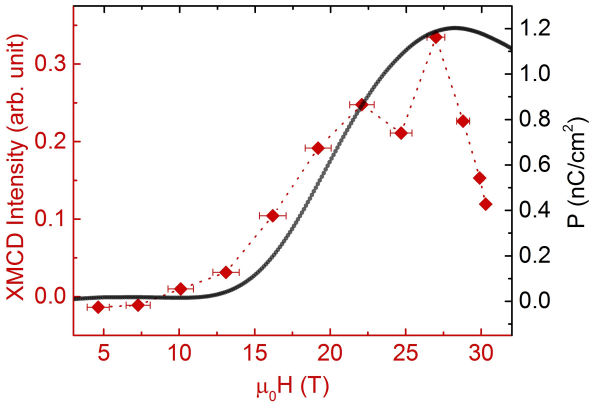

FIG. 3. Field dependence of the XMCD integrated intensity over the entire L_2-edge range at 2 K compared with the estimated field dependence of the electric polarization along the b-axis at T = 1.5 K shown in Fig.2. The dotted line is a guide to the eyes.

J_i	Ions involved	Distance (Å)	Magnitude (meV)
J_1	Mn^{4+}-Mn^{4+}	2.95	-0.110
J_2	Mn^{4+}-Mn^{4+}	2.74	0.118
J_3	Mn^{3+}-Mn^{4+}	3.39	-0.040
J_4	Mn^{3+}-Mn^{4+}	3.61	-0.004
J_5	Mn^{3+}-Mn^{3+}	3.61	-0.205
J_6	Pr^{3+}-Mn^{3+}	3.35	0.009

TABLE I. The Mn-Mn and Mn-Pr exchange interactions (in meV) obtained from the converged GGA+U calculations using the magnetic force theorem [38]. The negative value implies an antiferromagnetic interaction whereas the positive value implies a ferromagnetic one.

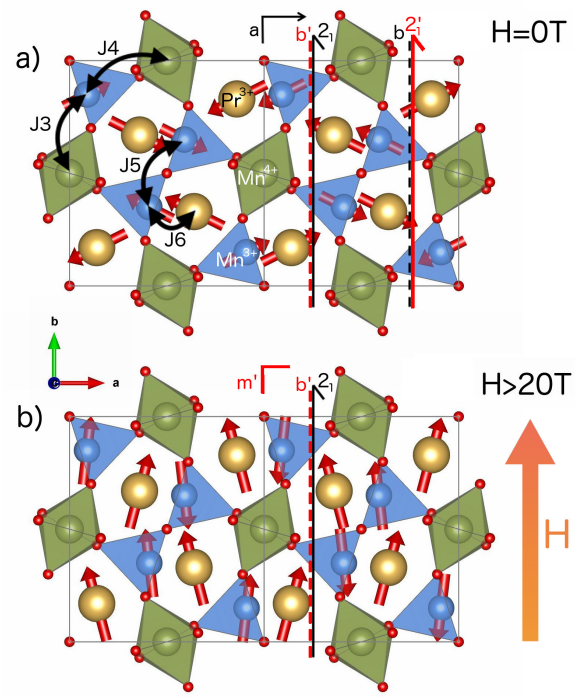

FIG. 4. Top: Schematic magnetic structure at zero field (magnetic space group P_ab2_1a). Bottom: Our proposed schematic magnetic structure at high field in the ferroelectric phase (magnetic space group $Pb'2_1m'$). Amplitude of the arrows showing magnetic moments are not normalized to the scale for the sake of clarity. Mn^{3+}, Mn^{4+}, and Pr^{3+} ions are represented in blue, green, and yellow respectively.

netic structure reported [24]. The interactions viz. J_3 to J_6 which play significant role in the present context are presented in Fig.4 along with the zero-field magnetic structure. The strongest interaction is J_5, imposing a perfect anti-parallel alignment of Mn^{3+} spins (represented in blue), along the direction of anisotropy. The Pr moments (in yellow) are only coupled to those Mn^{3+} through a ferromagnetic J_6. Owing to the perfect colinearity of Mn^{3+} and Pr^{3+} spins, it is reasonable to assume that Pr anisotropy is negligible compared to J_6. Now, it is easily understandable why Mn^{4+} (in green) moments are not coupled to the Mn^{3+} ones. Indeed, as can be seen in Table I, J_4 is two orders of magnitude smaller that J_5, excluding this path to connect the two sub-lattices. The other possible connection between Mn^{3+} dimers goes through J_3 interaction which is an order of magnitude smaller than J_5. This interaction connects Mn^{4+} to two perfectly antiparallel Mn^{3+} spins. As a consequence, the two paths connecting Mn^{3+} and Mn^{4+} via J_3 exactly compensate each other. As for J_1 (AF) and J_2 (F), they couple two Mn^{4+} moments along c. Symmetries of the magnetic structure are represented in Fig.4(a), resulting the magnetic space group P_ab2_1a. This space group is the same as the one reported for other members of the series such as $GdMn_2O_5$[10].

On the basis of the estimated exchange interactions, we propose a model to couple the experimentally observed ferromagnetic component of Pr^{3+} moments to the induced ferroelectricity along the b direction. As described earlier, the essential components responsible for the magnetic order are J_5 connecting $S_{Mn^{3+}}$ and $S_{Mn^{3+}}$ and J_6 connecting $S_{Mn^{3+}}$ and $S_{Pr^{3+}}$. Upon increasing the external magnetic field along the b direction, both $S_{Mn^{3+}}$ and $S_{Pr^{3+}}$ are expected to align along b. Due to the strong J_5 interaction, $S_{Mn^{3+}}$ will remain as an anti-parallel dimer. This dimer will rotate along b as soon as the magnetic field exceeds the anisotropy of Mn. For an anisotropy of less than 1 meV, we can expect it above 10 T. For Pr^{3+} moments, there is a competition between two opposite forces. In one hand, ferromagnetic J_6 interaction tries to align $S_{Pr^{3+}}$ spins parallel to the neighboring $S_{Mn^{3+}}$. As a consequence, Pr moments would be antiferromagnetically aligned like the $S_{Mn^{3+}}$ pairs. Now comes the Zeeman interaction term induced by the external magnetic field. It will push $S_{Pr^{3+}}$ to align along the b direction. As XMCD results show, the external magnetic field term becomes stronger than the J_6 interaction above ~12 Tesla, and a ferromagnetic component from Pr moments appears along b. A compatible magnetic structure preserving the maximum of the zero-field symmetries is schematically proposed in Fig.4(b). The magnetic symmetry operations (represented on the magnetic structure) correspond to the magnetic space group $Pb'2_1m'$ ($Pm'c'2_1$ #26.70

in conventional setting), a subgroup of $P_a b 2_1 a$. As a result, the two $S_{Mn^{3+}}$ - $S_{Pr^{3+}}$ pairs do not remain equivalent anymore. A slight displacement of oxygen ions bridging $S_{Mn^{3+}}$ and $S_{Pr^{3+}}$ is thus to be expected and would be different from one pair to the other. For the nearly ferromagnetically aligned pair, this displacement will tend to maximize the non-frustrated J_6 interaction. On the contrary, the oxygen displacement for the nearly antiferromagnetic pair will tend to minimize this J_6 exchange coupling. Displacements are thus different from one side to the other resulting an effective polarization along b as observed experimentally. From a structural point of view, the average centrosymmetric space group *Pbam* at zero field is no longer compatible. The high field space group is thus expected to be a non-centrosymmetric subgroup of *Pbam* and compatible with the $Pm'c'2_1$ Shubnikov group. Among the two possible subgroups fulfilling the first constraint (*Pba*2 and $Pmc2_1$), only $Pmc2_1$ allows a polarization along the b direction. Fortunately, this group also satisfies the second requirement since it is a subgroup of $Pmc2_11'$. As a conclusion, it is likely that the high field space group is $Pmc2_1$. This mechanism, leading to the coupling of ferromagnetic Pr component and ferroelectricity, is thus mediated purely by a 3*d*-4*f* superexchange interaction. This is fundamentally different from the exchange-striction mechanism involved in the other members of the family where a dominant 3*d*-3*d* interaction leads to the coupling between antiferromagnetism and ferroelectricity.

In conclusion, the combination of high-field electric polarization and XMCD measurements on $PrMn_2O_5$ single crystals along with the DFT calculations reveals emergence of SDFE under magnetic field with strong magnetoelectric coupling. In contrast to other RMn_2O_5 members (R = Nd to Lu), multiferroicity in $PrMn_2O_5$ under magnetic field is characterized by coexisting ferroelectric and ferromagnetic components. The underlying mechanism for this SDFE involves exchange-striction mechanism solely originated from 3*d*-4*f* coupling as opposed to the 3*d*-3*d* dominated multiferroicity in other members. The observation of such coupled ferroelectric-ferromagnetic state is highly interesting from the perspective of technological applications. The present study strongly indicates that there is possibility to stabilize a robust ferroelectric-ferromagnetic combination along with magnetoelectric coupling by manipulating the magnetic frustration using external parameters such as magnetic field or pressure. Further studies on other 3*d*-4*f* based frustrated magnets following this prescription would be highly beneficial.

We acknowledge the attribution of ESRF beam time under proposal HC-3783. We also acknowledge the support of the HLD at HZDR, member of the European Magnetic Field Laboratory (EMFL).

* s.chattopadhyay@hzdr.de

[1] N. Hur, S. Park, P. A. Sharma, J. S. Ahn, S. Guha, and S.-W. Cheong, Nature (London) **429**, 392 (2004).
[2] S. W. Cheong and M. Mostovoy, Nat. Mater. **6**, 13 (2007).
[3] M. Fiebig, T. Lottermoser, D. Meier, and M. Trassin, Nat. Rev. Mater. **1**, 16046 (2016).
[4] Y. Tokura, S. Seki, and N. Nagaosa, Rep. Prog. Phys. **77**, 076501 (2014).
[5] D. Khomskii, Physics **2**, 20 (2009).
[6] S. Chattopadhyay, V. Balédent, F. Damay, A. Gukasov, E. Moshopoulou, P. Auban-Senzier, C. Pasquier, G. André, F. Porcher, E. Elkaim, C. Doubrovsky, M. Greenblatt, and P. Foury-Leylekian, Phys. Rev. B **93**, 104406 (2016).
[7] G. Yahia, F. Damay, S. Chattopadhyay, V. Balédent, W. Peng, E. Elkaim, M. Whitaker, M. Greenblatt, M.-B. Lepetit, and P. Foury-Leylekian, Phys. Rev. B **95**, 184112 (2017).
[8] V. Polyakov, V. Plakhty, M. Bonnet, P. Burlet, L.-P. Regnault, S. Gavrilov, I. Zobkalo, and O. Smirnov, Physica B **297**, 208 (2001).
[9] G. R. Blake, L. C. Chapon, P. G. Radaelli, S. Park, N. Hur, S-W. Cheong, and J. Rodríguez-Carvajal, Phys. Rev. B **71**, 214402 (2005).
[10] G. Yahia, F. Damay, S. Chattopadhyay, V. Balédent, W. Peng, S. W. Kim, M. Greenblatt, M.-B. Lepetit, and P. Foury-Leylekian, Phys. Rev. B **97**, 085128 (2018).
[11] B Roessli, P. Fischer, P. J. Brown, M. Janoschek, D. Sheptyakov, S. N. Gvasaliya, B. Ouladdiaf, O. Zaharko, E. Golovenchits, and V. Sanina, J. Phys.: Condens. Matter **20**, 485216 (2008).
[12] M. Fukunaga, Y. Sakamoto, H. Kimura, Y. Noda, N. Abe, K. Taniguchi, T. Arima, S. Wakimoto, M. Takeda, K. Kakurai, and K. Kohn, Phys. Rev. Lett. **103**, 077204 (2009).
[13] Y. Noda, H. Kimura, M. Fukunaga, S. Kobayashi, I. Kagomiya, and K. Kohn, J. Phys.: Condens. Matter **20**, 434206 (2008).
[14] M. Fukunaga, Y. Sakamoto, H. Kimura, and Y. Noda, J. Phys. Soc. Jpn. **80**, 014705 (2011).
[15] I. Kagomiya and K. Kohn, Ferroelectrics, **219**, 169 (1998).
[16] P. G. Radaelli and L. C. Chapon, J. Phys.: Condens. Matter **20**, 434213 (2008).
[17] N. Hur, S. Park, P. A. Sharma, S. Guha, and S-W. Cheong, Phys. Rev. Lett. **93**, 107207 (2004).
[18] V. Balédent, S. Chattopadhyay, P. Fertey, M. B. Lepetit, M. Greenblatt, B. Wanklyn, F. O. Saouma, J. I. Jang, and P. Foury-Leylekian, Phys. Rev. Lett. **114**, 117601 (2015).
[19] I. Kagomiya, K. Kohn, and T. Uchiyama, Ferroelectrics **280**, 131 (2002).
[20] J. A. Alonso, M. T.Casais, M. J. Martinez-Lope, J. L. Martinez, and M. T. Fernandez-Diaz, J. Phys.: Condens. Matter **9**, 8515 (1997).
[21] S. Chattopadhyay, S. Petit, E. Ressouche, S. Raymond, V. Balédent, G. Yahia, W. Peng, J. Robert, M.-B. Lepetit, M. Greenblatt, and P. Foury-Leylekian, Sci. Rep. **7**, 14506 (2017).
[22] M. Deutsch, W. Peng, P. Foury-Leylekian, V. Balédent, S. Chattopadhyay, M. T. Fernandez-Diaz, T. C. Hansen, A. Forget, D. Colson, M. Greenblatt, M.-B. Lepetit, S. Petit, and I. Mirebeau, Phys. Rev. B **98**, 024408 (2018).
[23] S. Mansouri, S. Jandl, M. Balli, P. Fournier, B. Roberge, M. Orlita, I. A. Zobkalo, S. N. Barilo, and S. V. Shiryaev, Phys. Rev. B **98**, 205119 (2018).
[24] C. Doubrovsky, G. André, A. Gukasov, P. Auban-Senzier, C. R. Pasquier, E. Elkaim, M. Li, M. Greenblatt, F. Damay, and P. Foury-Leylekian, Phys. Rev. B **86**, 174417 (2012).
[25] W. Peng, V. Balédent, S. Chattopadhyay, M.-B. Lepetit, G. Yahia, C. V. Colin, M. J. Gooch, C. R. Pasquier, P. Auban-Senzier, M. Greenblatt, and P. Foury-Leylekian, Phys. Rev. B **96**, 054418 (2017).
[26] G. Popov, M. Greenblatt, and W. McCarroll, Mater. Res. Bull.

35, 1661 (2000).
[27] B. Wanklyn, J. Mater. Sci. **7**, 813 (1972).
[28] S. Pascarelli, O. Mathon, T. Mairs, I. Kantor, G. Agostini, C.Strohm, S. Pasternak, F. Perrin, G. Berruyer, P. Chappelet, C. Clavel, and M. C. Dominguez, J. Synchrotron Radiat. **23**, 353 (2016).
[29] P. van der Linden, O. Mathon, C. Strohm, and M. Sikora, Rev. Sci. Instrum. **79**, 075104 (2008).
[30] P. Frings, J. Vanacken, C. Detlefs, F. Duc, J. E. Lorenzo, M. Nardone, J. Billette, A. Zitouni, W. Bras, and G. L. J. A. Rikken, Rev. Sci. Instrum. **77**, 063903 (2006).
[31] C. Strohm, F. Perrin, M.-C. Dominguez, J. Headspith, P. vander Linden, and O. Mathon, J. Synchrotron Radiat. **18**, 224 (2011).
[32] A. M. G. Carvalho, F. Garcia, V. S. R. de Sousa, P. J. von Ranke, D. L. Rocco, G. D. Loula, E. J. de Carvalho, A. A. Coelho, L. M. da Silva, and F. C. G. Gandra, J. Magn. Magn. Mater. **321**, 3014 (2009).
[33] Y. E. Samoshkina and A. Rogalev, J. Exp. Theor. Phys. **126**, 660 (2018).
[34] J. Chaboy, M. A. Laguna-Marco, C. Piquer, R. Boada, H. Maruyama, and N. Kawamura, J. Synchrotron Radiat. **15**, 440 (2008).
[35] N. Kawamura, M. Suzuki, H. Maruyama, and T. Ishikawa, J. Synchrotron Radiat. **8**, 425 (2011).
[36] C. Strohm, P. van der Linden, O. Mathon, and S. Pascarelli, Phys. Rev. Lett. **122**, 127204 (2019).
[37] Y. O. Kvashnin, O. Grånäs, I. Di Marco, M. I. Katsnelson, A. I. Lichtenstein, and O. Eriksson, Phys. Rev. B **91**, 125133 (2015).
[38] M. I. Katsnelson and A. I. Lichtenstein, Phys. Rev. B **61**, 8906 (2000).